

THE MORPHOLOGY OF PASSIVELY EVOLVING GALAXIES AT $Z \sim 2$ FROM *HST*/WFC3 DEEP IMAGING IN THE HUBBLE ULTRADEEP FIELD¹

P. CASSATA², M. GIAVALISCO², YICHENG GUO², H. FERGUSON³, A. KOEKEMOER³, A. RENZINI⁴, A. FONTANA⁵, S. SALIMBENI², M. DICKINSON⁶, S. CASERTANO³, C. J. CONSELICE⁷, N. GROGIN³, J. M. LOTZ⁶, C. PAPOVICH⁸, R. A. LUCAS³, A. STRAUGHN⁹, J. P. GARDNER⁹, L. MOUSTAKAS¹⁰

Draft version May 31, 2019

ABSTRACT

We discuss near-IR images of six passive galaxies ($\text{SSFR} < 10^{-2} \text{ Gyr}^{-1}$) at redshift $1.3 < z < 2.4$ with stellar mass $M \sim 10^{11} M_{\odot}$, selected from the Great Observatories Origins Deep Survey (GOODS), obtained with WFC3/IR and the *Hubble Space Telescope* (*HST*). These WFC3 images provide the deepest and highest angular resolution view of the optical rest-frame morphology of such systems to date. We find that the light profile of these galaxies is generally regular and well described by a Sérsic model with index typical of today's spheroids. We confirm the existence of compact and massive early-type galaxies at $z \sim 2$: four out of six galaxies have $r_e \sim 1 \text{ kpc}$ or less. The WFC3 images achieve limiting surface brightness $\mu \sim 26.5 \text{ mag arcsec}^{-2}$ in the F160W bandpass; yet there is no evidence of a faint halo in the five compact galaxies of our sample, nor is a halo observed in their stacked image. We also find very weak “morphological k-correction” in the galaxies between the rest-frame UV (from the ACS z band), and the rest-frame optical (WFC3 H band): the visual classification, Sérsic indices and physical sizes of these galaxies are independent or only mildly dependent on the wavelength, within the errors.

Subject headings: cosmology: observations — galaxies: fundamental parameters — galaxies: evolution

1. INTRODUCTION

Most of the stellar mass observed in today's early-type galaxies has assembled at high redshifts ($z > 2$, see Renzini 2006). Thus, the evolution of the mass functions and morphology of these galaxies is expected to provide information on the mechanisms that have assembled and shaped them in their current state, e.g. merging and accretion.

Recent works agree that the most massive early-type galaxies (with $M/M_{\odot} > 10^{11}$) were already in place at $z \sim 1$, and characterized by a mass-dependent evolution of the luminosity function, whereas galaxies with lower mass evolve faster (Thomas et al. 2005; Franceschini et al. 2006; Bundy et al. 2006; Scarlata et al. 2007).

Galaxies at $1.5 < z < 3$ with stellar mass and SEDs similar to those of local early types have also been identified and studied thanks to a number of ded-

icated color-selection criteria (e.g. Franx et al. 2003; Daddi et al. 2004; Kong et al. 2006; Ilbert et al. 2009; McCracken et al. 2009), as well as spectroscopic surveys (e.g. Cimatti et al. 2008; Kriek et al. 2008). These galaxies have photometrically-measured stellar mass $m \sim 10^{11} M_{\odot}$ and specific star formation rate $\text{SSFR} < 10^{-2} \text{ Gyr}^{-1}$, nearly one order of magnitude lower than that of the Milky Way. There is broad agreement that the number density of these high-redshift “elliptical galaxies” rapidly increases from $z \sim 2$ to $z \sim 1$ (Fontana et al. 2006; Arnouts et al. 2007; Ilbert et al. 2009). The mechanisms through which they build up their mass, however, are not yet known. Especially intriguing is the recent discovery that at least some massive elliptical galaxies at $z > 1.5$ are, on average, $\sim 3\times$ smaller, and thus $\approx 30\times$ denser, than their local counterparts (Daddi et al. 2005; Trujillo et al. 2006; Trujillo et al. 2007; Zirm et al. 2007; Longhetti et al. 2007; Cimatti et al. 2008, Van Dokkum et al. 2008, Buitrago et al. 2008), a fact lacks an explanation in terms of evolutionary mechanisms (e.g. Hopkins et al. 2009a). Recent works (Valentinuzzi et al. 2009; Trujillo et al. 2009), however, have identified similarly dense massive galaxies in the local universe, although their spatial density seems smaller than the $z \sim 2$ galaxies.

Some have suggested that current observations at high redshift could have missed low surface-brightness halos surrounding these galaxies, due to the relatively limited sensitivity of current imaging data (Hopkins et al. 2009b; Mancini et al. 2009). If true, this could help explain the apparently dramatic morphological transformation of passive galaxies from $z \sim 2$ to the present. Another possibility is that current surveys of the local universe (e.g. the SDSS, Stoughton et al. 2002) could also have

¹ Based on data obtained with the *Hubble Space Telescope* operated by AURA, Inc. for NASA under contract NAS5-26555.

² Department of Astronomy, University of Massachusetts, Amherst, MA 01003; paolo@astro.umass.edu

³ Space Telescope Science Institute, 3700 San Martin Boulevard, Baltimore, MD, 21218

⁴ Osservatorio Astronomico di Padova (INAF-OAPD), Vicolo dell'Osservatorio 5, I-35122, Padova, Italy

⁵ INAF - Osservatorio Astronomico di Roma, via Frascati 33, Monteporzio-Catone (Roma), I-00040, Italy

⁶ NOAO-Tucson, 950 North Cherry Avenue, Tucson, AZ 85719

⁷ University of Nottingham, School of Physics and Astronomy, Nottingham NG7 2RD

⁸ George P. and Cynthia Woods Mitchell Institute for Fundamental Physics and Astronomy, Department of Physics, Texas A&M University, College Station, TX 77843-4242, USA

⁹ Astrophysics Science Division, Observational Cosmology Laboratory, Goddard Space Flight Center, Code 665, Greenbelt, MD 20771

¹⁰ Jet Propulsion Laboratory, California Institute of Technology, MS 169-327, Pasadena, CA 91109

missed a relatively large fraction of very compact, early-type galaxies due to the limited ground-based angular resolution (1 arcsec corresponds to a physical scale of ~ 1 kpc at $z = 0.05$).

A crucial step is to obtain an unbiased and statistically accurate measures of the size distribution of early-type galaxies at both high and low redshift (Cassata et al. in prep.). So far, while small high-redshift samples have been imaged with NICMOS at rest-frame optical wavelengths (Trujillo et al. 2007; Zirm et al. 2007; Longhetti et al. 2007; Van Dokkum et al. 2008), most of the galaxies only have rest-frame UV images from ACS and the dependence of the morphology of these galaxies on the wavelength has not been characterized (Cimatti et al. 2008; Daddi et al. 2005).

In this letter we use the unprecedented sensitivity and angular resolution of WFC3/IR images recently acquired in the HUDF to study the optical rest-frame morphology, as well as the spectral energy distributions, of a small but well defined sample of low SSFR galaxies at $z \sim 2$. The WFC3 images, in the Y, J and H bands (F105W, F125W and F160W, respectively) have PSF with FWHM=0.18" at 16000Å and reach $1 - \sigma$ surface brightness fluctuations of 27.2, 26.6 and 26.3 AB/arcsec², respectively, the sharpest and deepest ever obtained to date.

2. DATA ANALYSIS

The imaging data comprise the first epoch of ultra-deep near-IR WFC3/IR observations acquired by Bouwens et al. (2009, program ID=GO11563, P.I. G. Illingworth) in the HUDF (Beckwith et al. 2006), a $\approx 3.3 \times 3.3$ arcmin² field fully embedded in the GOODS-South field (Giavalisco et al. 2004) and imaged with the same photometric system, i.e. the ACS BViz. This first epoch of data covers an area roughly equal to the footprint of the WFC3/IR camera (2.1 arcmin²) and consists of images in the F105 (Y), F125W (J) and F160W (H) filters. We have carried out our independent reduction of the raw data and after rejecting images affected by persistence in the J band, our final stacks reach $1 - \sigma$ surface brightness fluctuations of 27.2, 26.6 and 26.3 in the three bands, respectively. The WFC3 images have been drizzled to a 0.06" pixel scale.

We selected a sample of high redshift ($z > 1.3$) passive (SSFR $< 10^{-2} \text{ Gyr}^{-1}$) and massive ($M > 10^{10} M/M_{\odot}$) galaxies from the GOODS multi-band GUTFIT photometric catalog by Grogin et al. (in preparation). This catalog contains matched photometry for all the photometric bands used for the GOODS multi-facility program from the U to the 8μm IRAC band (the MIPS 24μm photometry is not included). All our sample galaxies, however, have no detection at 24μm down to a $1 - \sigma$ limit of 5μJy. Fontana et al. (2009) have shown that it is possible to select a sample of passive galaxies at high- z combining MIPS 24μm to the optical-NIR spectral energy distribution. We used both the BzK color-selection criteria for passive galaxies by Daddi et al. (2004), as well as multi-band SED fitting to identify the sample. While the BzK technique provides a well characterized criterion to select galaxies with low specific star-formation rate (dubbed "pBzK", or passive BzK), the method naturally has finite completeness and contamination, since photometric errors and the intrinsic dispersion of galax-

ies' broad-band UV/Optical SED scatter galaxies out of the selection window and interlopers into it. Thus, given the overall limited size of the sample, we have augmented it with galaxies selected for being massive and passive according to the above criteria based on fitting their observed broad-band GUTFIT SED to stellar population synthesis models. We used the Charlot & Bruzual (2007) models with Salpeter IMF and lower and upper mass limits 0.1 and 100 M_{\odot} , respectively, together with the Calzetti et al. (2000) obscuration law to account for the possible (modest) presence of dust and the Madau (1995) cosmic opacity. The results of the SED fitting are reported in Table 1, and the SEDs are shown in Fig. 1.

The final sample, summarized in Table 1, consists of six galaxies, four of which have spectroscopic redshifts, i.e. 22704 and 23555 from Cimatti et al. (2008), 24279 from Daddi et al. (2005) and 24626 from Vanzella et al. (2008), and two for which we derived accurate ($\Delta z/(1+z) \sim 0.05$) photometric redshifts from the GUTFIT multi-band photometry. Four out of six galaxies fulfill the pBzK criterion.

We have used GALFIT (Peng et al. 2002) to fit the light profile of the galaxies in the z, Y, J and H bands to the Sérsic model

$$I(r) = I_e \exp \left\{ -b_n \left[\left(\frac{r}{r_e} \right)^{1/n} - 1 \right] \right\}, \quad (1)$$

where $I(r)$ is the surface brightness measured at distance r , I_e is the surface brightness at the effective radius r_e and b_n is a parameter related to the Sérsic index n . For $n=1$ and $n=4$ the Sérsic profile reduces respectively to an exponential or deVaucouleurs profile. Bulge dominated objects typically have high n values (e.g. $n > 2$) and disk dominated objects having n around unity. Cassata et al. (2005), Ravindranath et al. (2006) and Cimatti et al. (2008) showed that this method gives basically unbiased estimates of the Sérsic index and effective radius.

The star used by GALFIT to convolve the model has been obtained averaging six bright unsaturated stars in the UDF/WFC3 field. GALFIT has been run considering the sky as a free parameter and using a fitting region around each galaxy of 6×6 arcsec². However, we have run tests using a different region size and fixing the sky to different values, and the Sérsic indices and sizes so obtained were in agreement with the fiducial values within 20%.

3. THE MORPHOLOGICAL PROPERTIES OF GALAXIES AT $Z \sim 2$.

Figure 1 shows for each galaxy the z - and H -band images, the H -band residuals after subtracting the best GALFIT model and the model and galaxy profiles, together with the SEDs. Recall that at $z \sim 2$, the z band probes the rest-frame UV and the H band rest-frame optical.

Even on visual inspection, all the galaxies except 24646 appear to be very compact. In Fig. 1 the H -band images seem to be larger than the z -band ones, but this is just the result of the broader PSF (FWHM=0.16" in the H band vs. FWHM=0.12" in z). The light profiles in both passbands are actually rather similar. At all wavelengths, all galaxies appear relatively symmetric,

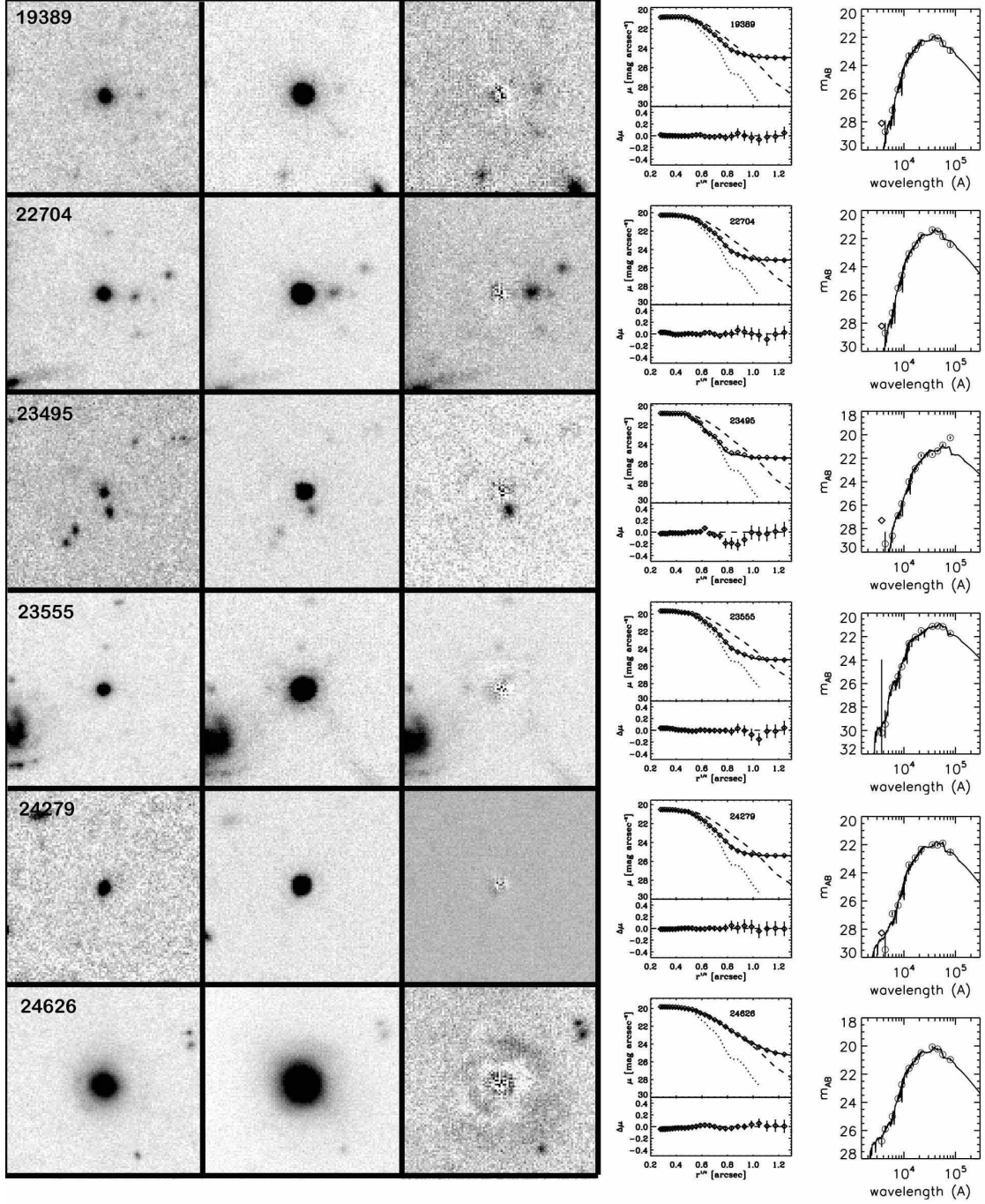


FIG. 1.— For each galaxy in the sample we show the postage stamp in z -band (1st column), in H -band (2nd column) and the residual after subtracting the best fit model in H -band (3rd column). Each postage stamp is 6×6 arcsec². In the 4th column, we show the galaxy profile in H -band, overplotted to the profile of the PSF (dotted line) and a de Vaucouleurs profile with $r_e = 3kpc$ (dashed line), together with the residual between galaxy and model profiles (bottom). Finally, in the 5th column we report the SED with the photometric best-fit model.

in close resemblance to present-day spheroidal galaxies. The only exception is galaxy 24626, the most extended of our sample, whose isophotes deviate from an elliptical one. A low surface brightness shell-like structure is visible in the z -band image, on the lower-left side, while the position angle is different for different isophote levels. These irregularities can be the result of ongoing or recent interactions.

The GALFIT Sérsic indices and sizes from the H -band

images are listed in Table 1; they quantitatively validate the conclusions derived from the visual inspection. Of the six galaxies, four have Sérsic index $\gtrsim 2$ (19389, 22704, 23555 and 24626). In the case of object 19389 we had to add a central unresolved (PSF) component to the Sérsic model to obtain a reasonable fit. This central stellar object contains less than 10% of the total light in the object, and may be indicative of an AGN. Galaxy 23495 also has a peculiar morphology: based on the FWHM, the object

TABLE 1
THE SAMPLE OF PASSIVE GALAXIES

ID	$z^{(1)}$	$\log(M/M_{\odot})$	$\log(\text{SSFR})$ [Gyr^{-1}]	Sérsic H-band	r_e [kpc]
19389	1.307p	10.41	-5.55	2.99 ⁽²⁾	1.02 ⁽²⁾
22704	1.384s	10.70	-5.55	2.65	0.50
23495	2.349p	11.14	-3.39	⁽³⁾	< 0.38
23555	1.921s	10.82	-2.98	1.97	0.44
24279	1.980s	10.63	-3.39	1.63	0.37
24626	1.317s	11.10	-2.11	7.42	3.69

NOTE. — (1): *s* and *p* indicate respectively spectroscopic and photometric redshifts; (2) the morphology of this object is reproduced by adding to the Sérsic model a central psf component; (3) the morphology of this object is reproduced by a single central psf component, so the size reported here is just an upper limit.

is barely resolved in all bands, Fig. 1 shows that the inner part of the galaxy’s profile ($r \lesssim 1$ arcsec) follows quite well the PSF profile, while the GALFIT best fit is that of an unresolved (PSF) light profile, again suggesting the presence of an AGN. Object 23495 is indeed detected in the Chandra Deep Field South 2-Megasecond Catalog (Luo et al. 2008), in both the X-ray channels. The luminosities are $3.2 \times 10^{43} \text{ erg/s}$ and $4.8 \times 10^{43} \text{ erg/s}$ respectively in the soft and hard band. On the contrary, object 19389 is not detected. Object 24279 has a Sérsic index of intermediate value $n \sim 1.6$, suggesting that this is probably a bulge dominated disk galaxy. Finally, to obtain a reasonable fit to object 24626, we had to use a combination of two components: one Sérsic model with a very high Sérsic index to reproduce the inner part of the galaxy, and a second one with $n \sim 1$ to reproduce the outskirts.

It is also interesting to analyze the residual maps produced by subtracting the best-fit model from the original image to investigate the presence of diffuse low-surface brightness halos, as recently suggested by some (Mancini et al. 2009; Hopkins et al. 2009b). The residual maps show some residual noise in the inner $0.5''$: this is because we are using an averaged PSF, but the actual PSF is not homogeneous across the field. However, this effect does not produce any systematic bias in the fitting procedure, as it can be seen looking at the 4th column of Fig. 1. It is evident that in none of our galaxies such a halo is observed. The only exception could be the case of galaxy 24626, which requires a two-component model to reproduce its light profile, an inner bulge-like part and an outer disk. Subtracting both of these two components, however, leaves a complex residual map, revealing a substantially more irregular light distribution compared to the other galaxies. Finally, note that both components have effective radius $r_e \sim 3$ kpc, implying that even if observed in shallower images that miss the low surface brightness component, the effective radius would still be found to be ~ 3 kpc.

To further explore the possible presence of a faint halo around these galaxies we have stacked together all of them except galaxy 24626 and then fitted the stacked image with GALFIT following the same procedure used for individual galaxies. The stacked image, which also looks very compact, and the GALFIT residual map are shown in Figure 2. The residual image, consistent with what we have found analyzing the individual galaxies, does not show any large-scale diffuse halo (close com-

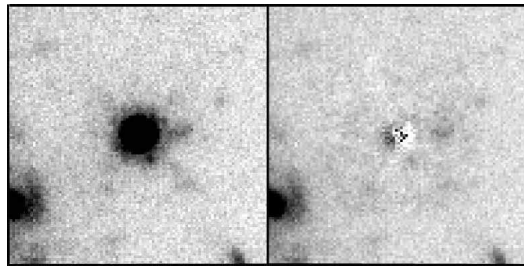


FIG. 2.— Stack for the 5 compact galaxies (19389, 22704, 23495, 23555, 24279) galaxies in the sample (*left panel*), and residuals after subtracting a Sérsic model (*right panel*).

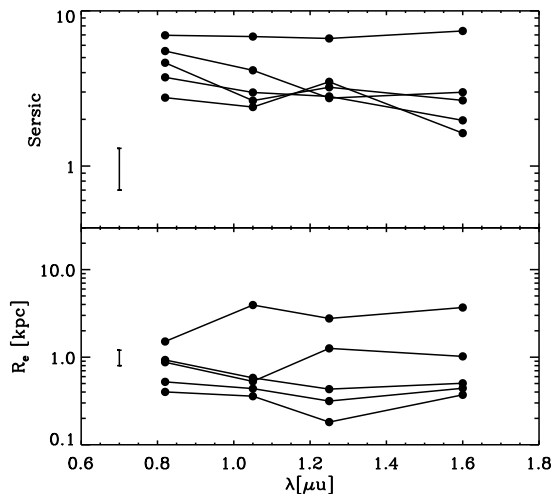


FIG. 3.— For the 5 galaxies in the sample best fitted by a Sérsic model, we show the Sérsic index (*upper panel*) and the effective radius (*bottom panel*) as a function of the wavelength. Object 23495, that is best-fitted by a point like source, is not reported in this figure. The typical error bars are shown, and amount to about 30% on the Sérsic indices and to about 20% on sizes.

panions have not been masked before the stack and have not been fitted). For all the galaxies and for the stacked image, however, the amount of residual light in the inner $2''$ is lower than 2% of the total light in the galaxy within the same aperture.

In Figure 3 we compare the Sérsic profiles in the *z*, *Y*, *J* and *H* bands, sampling the morphology from the rest-frame UV at $\lambda \sim 3300 \text{ \AA}$ to the optical one at $\sim 6000 \text{ \AA}$ (assuming mean redshift $\langle z \rangle = 1.7$). Consistent with our visual inspection, this shows weak or no evidence of morphological *k*-correction, since the Sérsic indices only slightly decrease from the *z* through the *H* band, implying only a slight higher more compact morphology at bluer wavelengths than at redder ones. This is in agreement with reports that the morphology of elliptical galaxies is largely independent of the wavelength (Pavovich et al. 2003; Cassata et al. 2005).

Similarly, the effective radius of all the six galaxies in our sample does not depend on the wavelength (see bottom panel of Fig. 3), with two of them showing no dependence of the size on the wavelength within the errors, and three showing a slight, but statistically signifi-

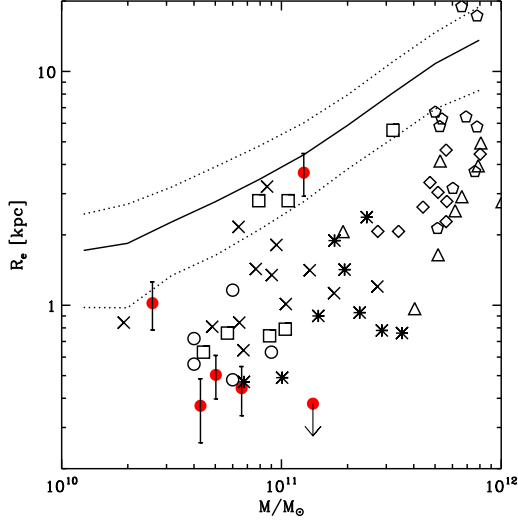


FIG. 4.— The distribution of effective radii versus stellar mass for galaxies in our sample (red filled circles). The continuous and dashed lines represent the local relation and its scatter, from Shen et al. (2003). Galaxy 23495 is shown as an upper limit, since its best-fit is a stellar-like profile. Crosses, circles, squares, stars, triangles, pentagons and diamonds indicate the early-types of Cimatti et al. (2008), Zirm et al. (2007), Daddi et al. (2005), Van Dokkum et al. (2008), Trujillo et al. (2006), Mancini et al. (2009) and Longhetti et al. (2007). Mass measurements have been homogenized to CB07 models and Salpeter IMF.

cant, decrease with increasing wavelengths, being $\sim 40\%$ smaller in H band than in the z one. This results in a negative color gradient, with the outer part of the galaxies being bluer than the center. This color gradient has also been measured by Guo et al. (in preparation) using aperture photometry, and they report that SED fitting shows that the properties of the stellar populations in the outer parts of these passive galaxies are, on average, ~ 0.5 Gyr younger than those in the center. We conclude by noting that the mild dependence of the morphology of our galaxies on wavelength is in good agreement with other studies of early-type galaxies at high-redshift from ACS and NICMOS images (McCarthy et al. 2007; Trujillo et al. 2007).

4. THE MASS-SIZE RELATION AT $Z \sim 2$

In Figure 4 we compare the relationship between mass and size (in the H band) for the six galaxies in our sample to other measures and to local galaxies (see figure caption). The mass measurements have been homogenized to CB07 and Salpeter IMF, applying typical offsets: we used $M_{CB07} = M_{BC03} - 0.2$ and $M_{Salp} = M_{Chab} + 0.25$ (Salimbeni et al. 2009). Four out of our six galaxies are located below the local relation for early-type galaxies, in agreement with other reports that massive galaxies at $z \sim 2$ are significantly more compact than their local counterparts. The remaining two (19389, the object with a stellar component at the center, and 24626, the large elliptical with multiple components) are on the local relation. We find it intriguing that these two galaxies also are the ones with the lowest redshift in our sample.

Thus, the sample that we have discussed here confirms the existence of very compact and dense passive galaxies at ~ 2 , on average about 3 to 5 times smaller and about 50–100 times denser than local counterparts, reported by

other authors from similar but shallower and/or lower quality images (Trujillo et al. 2007; Zirm et al. 2007; Longhetti et al. 2007; Van Dokkum et al. 2008) or at UV rest-frame wavelengths (Daddi et al. 2005; Cimatti et al. 2008). It, however, also suggests a diversity of morphological properties (size and stellar mass density) among these galaxies, with some of them, possibly the ones detected at lower redshifts (i.e. $1.3 < z < 1.5$) being rather similar to those observed in the local universe.

5. CONCLUSIONS

We have studied the UV and optical rest-frame morphology of 6 passively evolving galaxies $1.3 < z < 2.4$, four of which have spectroscopically confirmed redshifts.

The galaxies have on average a relatively smooth and regular morphology, which only mildly depends on wavelength. Based on visual inspection and on the analysis of the azimuthally averaged light profile, which is relatively well described by a Sérsic profile, we classify the six galaxies as early types. This is consistent with their selection, which is solely based on their broad-band SED, suggesting a tight correlation between spectral and morphological properties in close similarity to what is observed in the local universe, i.e. the Hubble sequence. Two of our galaxies appear to include a spatially unresolved (at the resolution afforded by the combination of *HST* and WFC3/IR) source at the center that could be indicative of an AGN. For one galaxy, object 23495, the central point source is responsible for the bulk of the observed luminosity in the H-band, and this object is in fact detected with Chandra, having $L_X \sim 3.5 \times 10^{43} \text{ erg/s}$.

Overall the Sérsic analysis yields similar results regardless of the bandpass indicating that for these galaxies the morphological k-correction between the rest-frame UV and optical is small. This particular property opens the possibility to study the morphology of these galaxies using large, deep and well-controlled samples available from the optical images of the GOODS and other similar surveys. We plan to report on such studies in a forthcoming paper (Cassata et al. in preparation), where we compare the distribution of mid-UV morphology of ~ 150 passive galaxies at $z \sim 2$ from GOODS (z band) with those of local early-type galaxies from the SDSS at the same rest-frame wavelength (u band).

We do not see any evidence of a faint halo surrounding the compact core of these galaxies, neither in the individual residuals (after subtracting the best-fit Sérsic profile), nor in stacked images, for five out of six galaxies in our sample. One galaxy, object 24626, requires at least two components to provide a good fit, one Sérsic model with high n (spheroid) embedded in a low surface brightness disk. Curiously, both components have similar effective radius (but different luminosity), both in the z and H bands, implying that in shallower surveys that miss the extended component the measured effective radius would be the same as the one we derived from the very deep WFC3 images.

Four out of six galaxies in our sample lie below the local mass-size relation for early-type galaxies, confirming previous reports that such galaxies at $z \sim 2$ can be ~ 3 times more compact at a given mass and thus ~ 50 times denser than locally. One of our galaxies, however (object 19389), which likely has an unresolved cen-

tral component, is on the boundary of the local relation, while another (object 24626) is well within the local relation. Thus, the deep WFC3 images also show, as suggested in other previous studies (Cimatti et al. 2008;

Mancini et al. 2009) that there are early-type galaxies at $z > 1.5$ with size and mass similar to those of local counterparts.

REFERENCES

- Arnouts, S. et al. 2007, *A&A*, 476, 137
 Beckwith, S. V. W. et al. 2006, *AJ*, 132, 1729
 Buitrago, F., et al. 2008, *ApJ*, 687, 61L
 Bundy, K., et al. 2006, *ApJ*, 651, 120
 Calzetti, D., et al. 2000, *ApJ*, 533, 682
 Cassata, P., et al. 2005, *A&A*, 357, 903
 Cimatti, A., et al. 2008, *A&A*, 482, 21
 Daddi, E., et al. 2004, *ApJ*, 617, 746
 Daddi, E., et al. 2005, *ApJ*, 626, 680
 Fontana, A., et al. 2006, *A&A*, 459, 745
 Fontana, A., et al. 2009, *A&A*, 501, 15
 Franceschini, A., et al. 2006, *A&A*, 453, 397
 Franx, M., et al. 2003, *ApJ*, 587, 79
 Giavalisco, M., et al. 2004, *ApJ*, 600, L93
 Hopkins, P. F., et al. 2009, [astro-ph/0909-2039]
 Hopkins, P. F., et al. 2009, *MNRAS*, 398, 898
 Ilbert, O., et al. 2009, [astro-ph/0903-0102]
 Longhetti, M., et al. 2007, *MNRAS*, 374, 614
 Luo, B., et al. 2008, *ApJS*, 179, 19
 Kong, X., et al. 2006, *ApJ*, 638, 72
 Kriek, M., et al. 2007, *ApJ*, 677, 219
 McCracken, H. J., et al. 2009, [astro-ph/0910-2705]
 Mancini, C., et al. 2009, [astro-ph/0909-3088]
 Madau, P., 1995, *ApJ*, 441, 18
 Papovich, C., et al. 2003, *ApJ*, 598, 827
 Peng, C. Y., et al. 2002, *AJ*, 124, 266
 Renzini, A., 2006, *ARA&A*, 44, 141
 Salimbeni, S., et al. 2009, American Institute of Physics Conference Series, Vol. 1111, 207
 Scarlata, C., et al. 2007, *ApJS*, 172, 494
 Shen, S., et al. 2003, *MNRAS*, 343, 978
 Stoughton, C., et al. 2002, *AJ*, 123, 485
 Thomas, D., et al. 2005, *ApJ*, 621, 673
 Trujillo, I., et al. 2006, *MNRAS*, 373, L36
 Trujillo, I., et al. 2007, *MNRAS*, 382, 109
 Van Dokkum, P. G., et al. 2008, *ApJ*, 677, L5
 Valentinuzzi, T., et al. 2009, [astro-ph/0907-2392]
 Vanzella, E., et al. 2008, *A&A*, 478, 83
 Zirm, A. W., et al. 2007, *ApJ*, 656, 66